JMEPEG (2017) 26:465–471
DOI: 10.1007/s11665-016-2462-0

1059-9495/$19.00

Solution and Aging of MAR-M246 Nickel-Based Superalloy

Renato Baldan, Antonio Augusto Araújo Pintoda Silva, Carlos Angelo Nunes, Antonio Augusto Couto, Sinara Borborema Gabriel, and Luciano Braga Alkmin

(Submitted June 1, 2016; in revised form September 23, 2016; published online December 9, 2016)

Solution and aging heat-treatments play a key role for the application of the superalloys. The aim of this work is to evaluate the microstructure of the MAR-M246 nickel-based superalloy solutioned at 1200 and 1250 °C for 330 min and aged at 780, 880 and 980 °C for 5, 20 and 80 h. The γ′ solvus, solidus and liquidus temperatures were calculated with the aid of the JMatPro software (Ni database). The as-cast and heat-treated samples were characterized by SEM/EDS and SEM-FEG. The γ′ size precipitated in the aged samples was measured and compared with JMatPro simulations. The results have shown that the sample solutioned at 1250 °C for 330 min showed a very homogeneous γ matrix with carbides and cubic γ′ precipitates uniformly distributed. The mean γ′ size of aged samples at 780 and 880 °C for 5, 20 and 80 h did not present significant differences when compared to the solutioned sample. However, a significant increasing in the γ′ particles was observed at 980 °C, evidenced by the large mean size of these particles after 80 h of aging heat-treatment.

Keywords aging, heat-treatment, MAR-M246, microstructure, solution, superalloy

1. Introduction

The MAR-M246 is a polycrystalline nickel-cobalt-tungsten superalloy developed by Martin Marietta Corporation, which became part of Lockheed Martin Inc. (USA) in 1995. This superalloy has been widely employed in rotors of automotive turbochargers and in high-pressure turbo pumps (Ref 1). The density of MAR-M246 superalloy is 8.44 g/cm^3 and the melting range is between 1315 and 1345 °C (Ref 2). The MAR-M246 superalloy generally solidifies with a dendritic structure containing carbides and exhibits extensive interdendritic segregation. A variant alloy, called MAR-M246 (Hf), contains 1.5 wt.% hafnium, which is added as a carbide former and grain boundary strengthener. The as-cast microstructure contains carbides and the gamma (γ)-gamma prime (γ′), eutectic, as well as the nickel-based matrix which is strengthened by solid-state precipitated γ′ phase (Ref 3).

Solution heat-treatments are commonly used for nickel-based superalloys and play a key role for the application of these materials at high temperatures (Ref 4, 5). The purpose of this heat-treatment is to solutionize the γ′ phase in the γ matrix and eliminate segregation generated due to non-equilibrium solidification (Ref 6). Then, aging heat-treatments are applied to provide higher creep resistance by generating very fine secondary γ′ particles with suitable size and distribution in the γ matrix (Ref 7-11). To achieve the best results in terms of mechanical properties, the temperature and duration of these heat-treatments must be carefully controlled.

The creep-rupture strength of superalloys is one of the most significant properties to consider during the material selection process. The high-temperature (760-1200 °C) creep-rupture characteristics of nickel-based superalloys are superior to those of either cobalt or nickel-iron-based superalloys. Cast nickel-based superalloys such as MAR-M246 maintain high stress-rupture strengths at elevated temperatures. (Ref 12, 13).

The aim of this work is to present the microstructural evolution of MAR-M246 superalloy submitted to different solutioning and aging heat-treatments conditions, correlating and comparing the results with simulations from JMatPro software.

2. Experimental Procedure

The nominal composition of the MAR-M246 nickel-based superalloy employed in this work is (wt.%): 10 Co; 10 W; 9 Cr; 5.5 Al; 2.5 Mo; 1.5 Ti; 1.5 Ta; 0.15C; 0.05 Zr; 0.015 B; Ni balance. Samples were extracted from the central part of turbo charger rotors via electro-discharge machining for the heat-treatment experiments. These samples were encapsulated in

Renato Baldan, São Paulo State University (Unesp), Campus of Itapeva, Rua Geraldo Alckmin 519, Itapeva, São Paulo, 18409-010, Brazil; **Antonio Augusto Araújo Pinto da Silva**, Instituto de Engenharia Mecânica - IEM, Universidade Federal de Itajubá - UNIFEI, Avenida BPS 1303, Itajubá, MG 37500-903, Brazil; **Carlos Angelo Nunes**, Escola de Engenharia de Lorena (EEL), Departamento de Engenharia de Materiais (DEMAR), Universidade de São Paulo (USP), Estrada Municipal do Campinho, Lorena, São Paulo 12602-810, Brazil; **Antonio Augusto Couto**, Instituto de Pesquisas Energéticas e Nucleares (IPEN), Av. Lineu Prestes, 2242, Cidade Universitária, 05508-000 São Paulo, Brazil; **Sinara Borborema Gabriel**, Faculdade de Tecnologia de Resende, UERJ – Universidade do Estado do Rio de Janeiro, Rodovia Presidente Dutra km 298 (sentido RJ-SP) - Pólo Industrial, 27537-000 Resende, Rio de Janeiro, Brazil; and **Luciano Braga Alkmin**, Campus Angra dos Reis, CEFET-RJ - Centro Federal de Educação Tecnológica Celso Suckow da Fonseca, Rua do Areal, 522, 23953-030 Angra dos Reis, Rio de Janeiro, Brazil. Contact e-mail: renatobaldan@gmail.com.

quartz tubes under argon atmosphere (min. 99.995%) and then heat-treated in a tubular furnace followed by air cooling. The solution heat-treatments were performed at 1200 and 1250 °C for 5.5 h while the aging heat-treatments were performed at 780, 880 and 980 °C for 5, 20 and 80 h. A K-type thermocouple was placed near the sample to determine accurately the true temperature of the materials. The heat-treatment conditions were chosen based on data of liquidus, solidus and γ' solvus temperatures determined from simulations using the JMatPro software (Ni database).

For microstructural characterization, the samples were prepared following conventional metallographic techniques and etched with an aqueous solution of 1% citric and 1% ammonium persulfate. The microstructural analysis was performed with the aid of a conventional scanning electron microscope (SEM) Hitachi TM 3000 with OXFORD Swift ED3000EDS detector and a field emission gun scanning electron microscope (FEG-SEM) JEOL JSM-6701F. The hardness values of all samples were determined using a Buehler Micromet equipment applying a load of 500 gf for 30 s.

The γ' mean diameters of aged samples were measured directly from the micrographs (approximately 2000 particles randomly distributed) with the aid of ImageJ software. The shape of each particle was approximated to a square and an equivalent diameter was calculated by the relationship $A = \pi d^2/4$, where A is the area of the square and d is the equivalent diameter of the particle.

3. Results and Discussions

3.1 Thermodynamic Simulations with JMatPro

Figure 1 shows the simulation of phase amount (wt.%) between 600 and 1400 °C for the MAR-M246 superalloy. It

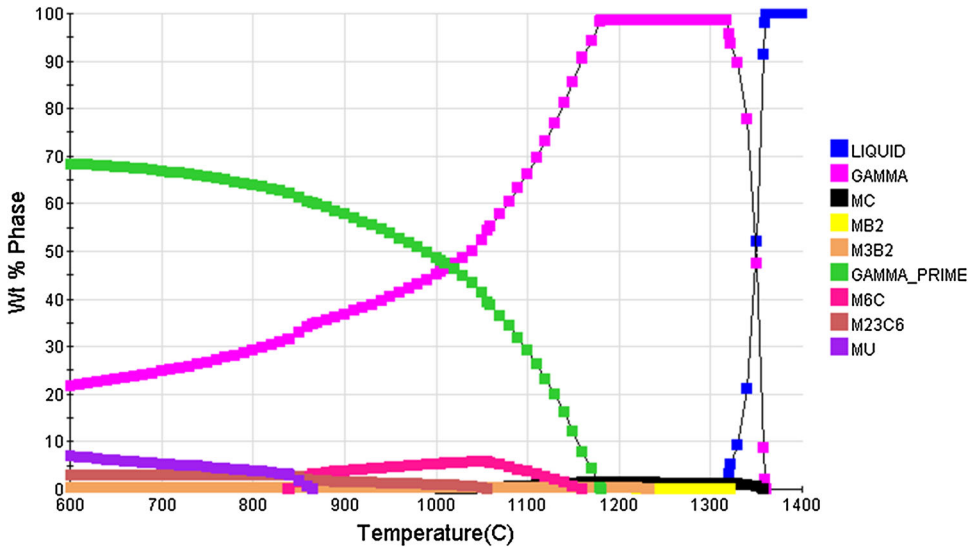

Fig. 1 Simulation of phase amount (wt.%) between 600 and 1400 °C for the MAR-M246 superalloy

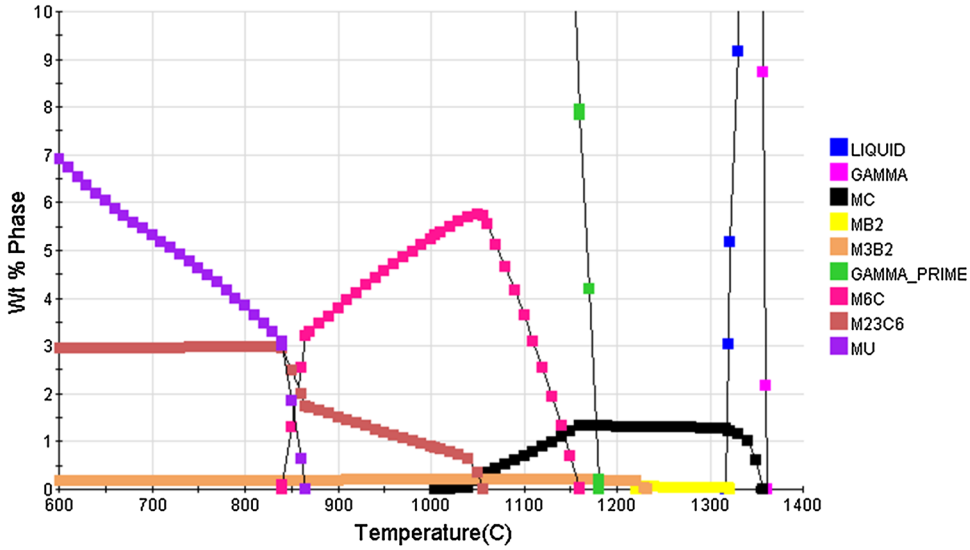

Fig. 2 Simulation of amount of minor phases (wt.%) between 600 and 1400 °C for the MAR-M246 superalloy

Table 1 Amount of phases for MAR-M246 nickel-based superalloy at 780, 880 and 980 °C

Temperature, °C	Phases, wt.%				
	γ′	M_3B_2	$M_{23}C_6$	M_6C	μ
980	50.8	0.2	1.0	5.0	0
880	59.1	0.2	1.7	3.5	0
780	64.6	0.2	3.0	0	4.2

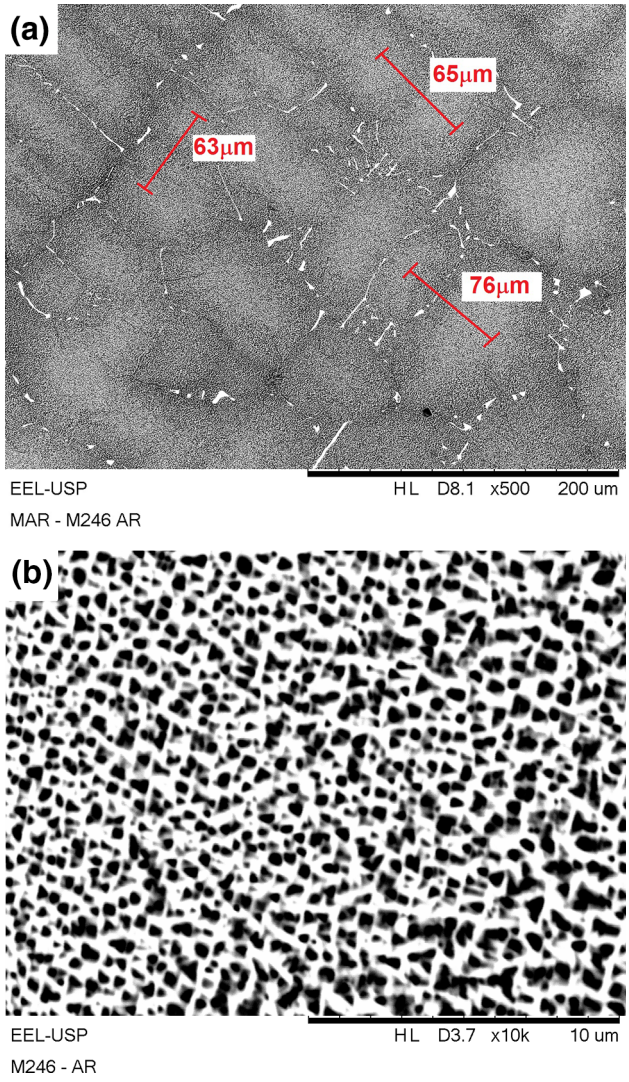

Fig. 3 (a) Microstructure of the as-cast MAR-M246 nickel-based superalloy. (b) Microstructure of the as-cast MAR-M246 nickel-based superalloy

can be seen that γ phase and MC carbides precipitate almost simultaneously near 1360 °C, γ being the primary phase. The liquidus, solidus and γ′ solvus temperatures are 1361, 1317 and 1181 °C, respectively. Based on this, on equilibrium conditions the temperature range for solution heat-treatment of the MAR-M246 superalloy is between 1181 and 1317 °C. It should be pointed out that in this range the alloy is not γ single-phase, being also composed of MC carbide and M_3B_2/MB_2 boride phases. Figure 2 shows the amount of minor phases from JMatPro simulations for the same temperature range. For the solution temperature range (between 1181 and 1317 °C), it can be seen that the MC carbide is stable and does not decompose while the MB_2 boride decomposes and forms the M_3B_2 boride near 1230 °C. In addition, other phases ($M_{23}C_6$ and M_6C carbides, M_3B_2 boride and μ phase) may be present in the lower temperature region of aging treatment (between 780 and 980 °C). Table 1 shows the simulation (JMatPro software) of expected amount of phases at 780, 880 and 980 °C. The amount of γ′ and $M_{23}C_6$ phases increases and that of M_6C carbide decreases as the aging temperature is reduced. Finally, the γ′ fraction for MAR-M246 superalloy decreases from 64.6 wt.% at 780 °C to 59.1 wt.% at 880 °C and 50.8 wt.% at 980 °C.

3.2 Microstructural Characterization of the As-Cast Material

Figure 3(a) shows the as-cast microstructure of MAR-M246 nickel-based superalloy. It can be seen a segregated dendritic microstructure and MC carbides in the interdendritic regions, with different sizes and morphologies. The mean value of primary dendrite arm spacing (3 measurements) is about 68 μm. As expected, γ′ precipitates formed via a solid-state reaction during cooling were observed in the primary γ dendrites, as depicted in Fig. 3(b), associated with a decrease in aluminum and titanium solubility in γ at lower temperatures. Standardless EDS analysis of the MC carbide phase (13 measurements) identified the main metallic elements present as follow (in wt.%): 27.4 ± 4.3 Ti, 8.6 ± 0.8 Cr, 8.3 ± 1.6 Mo, 10.9 ± 1.9 Ta, 12.7 ± 2.3 W (C removed from the quantification). Other elements are Ni (24.0 ± 2.5), Al (3.4 ± 0.4) and Co (4.7 ± 0.5) which were detected likely due to matrix effect on the EDS measurement. The EDS x-ray mapping from the carbide phase is shown in Fig. 4. Despite the presence of borides from the JMatPro simulations results, they were not detected in the samples, possibly because of their very small amount and size.

3.3 Microstructural Characterization of Solutioned Samples

It was possible to note an important effect of a 50 °C temperature increase in the microstructures, by comparing the samples solutioned at 1200 °C (Fig. 5a) and 1250 °C for 330 min (Fig. 5b). Evidences of segregation in the dendritic regions are still observed after heat-treated at 1200 °C for 330 min. However, the microstructure of the alloy heat-treated at 1250 °C for 330 min shows a homogeneous γ matrix with carbides.

Figure 6(a) and (b) shows the γ′ phase in the samples heat-treated at 1200 and 1250 °C for 330 min, respectively, noting some γ′ clusters in the sample heat-treated at 1200 °C. At the solution heat-treatment temperature, the primary γ′ particles from the as-cast microstructure begins to break down and dissolves gradually into smaller particles known as secondary γ′ up to the complete γ′ phase dissolution, leading to an

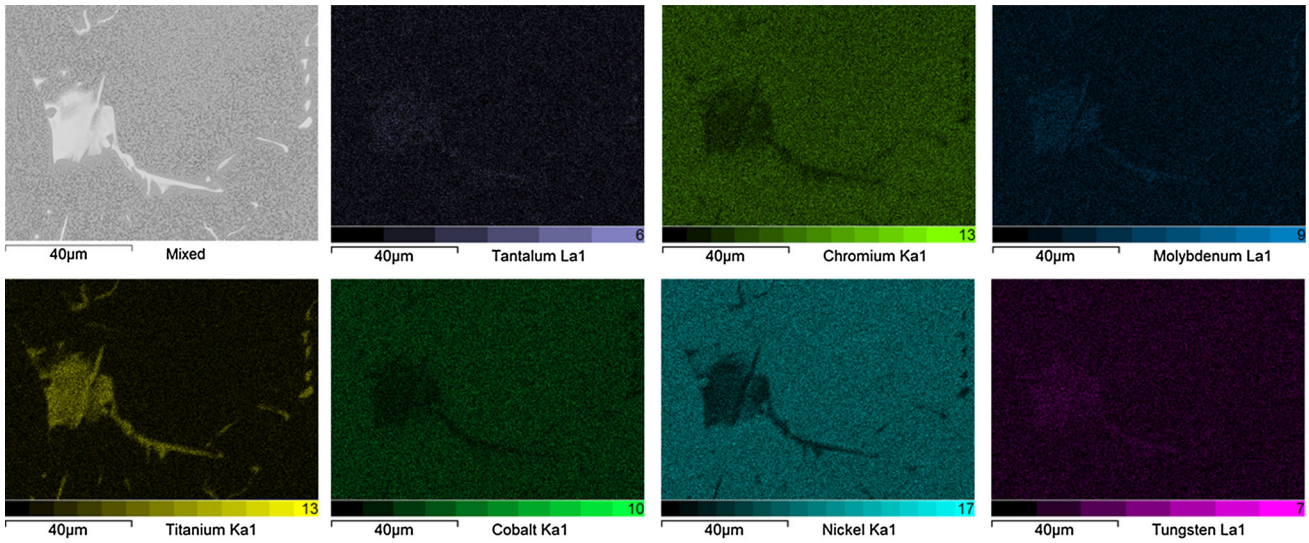

Fig. 4 EDS mapping of the carbide on the microstructure of the as-cast MAR-M246 superalloy

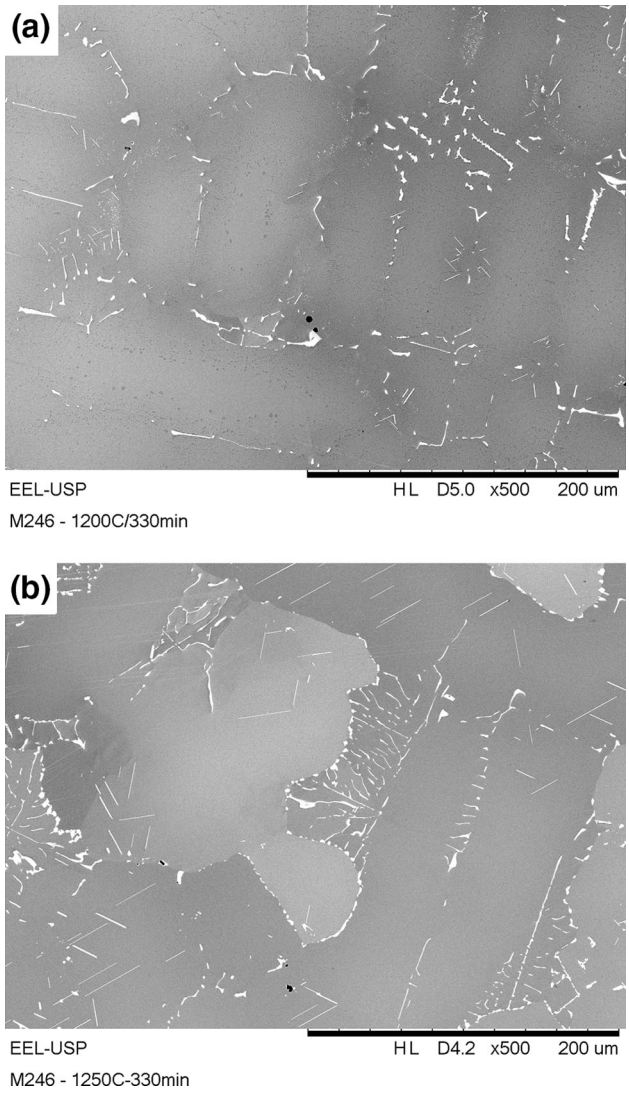

Fig. 5 Microstructure of the samples heat-treated at: (a) 1200 °C for 330 min (b) 1250 °C for 330 min

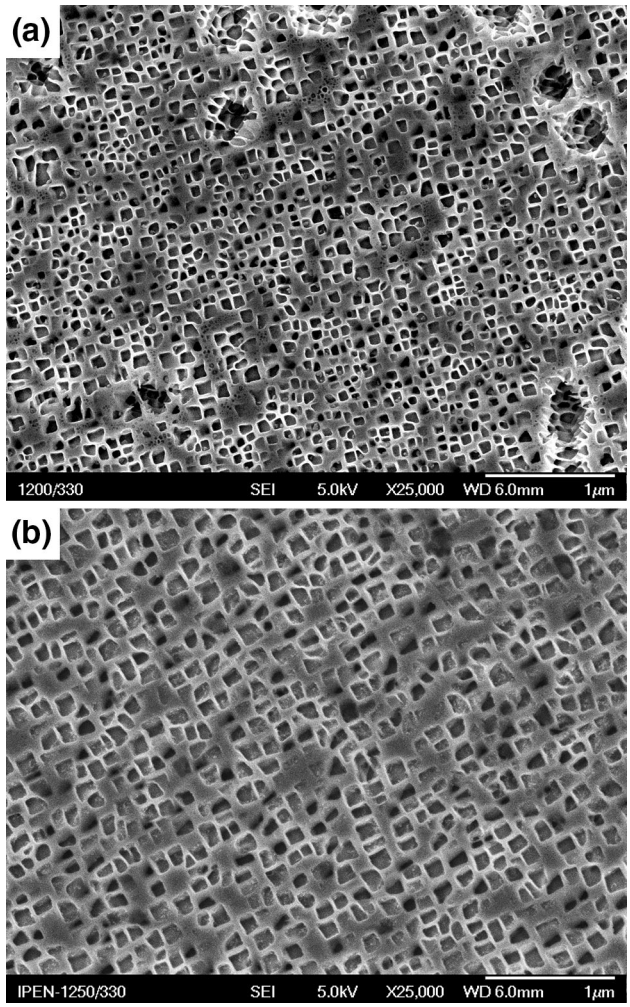

Fig. 6 γ' phase in the microstructure of the sample heat-treated at: (a) 1200 °C for 330 min (b) 1250 °C for 330 min

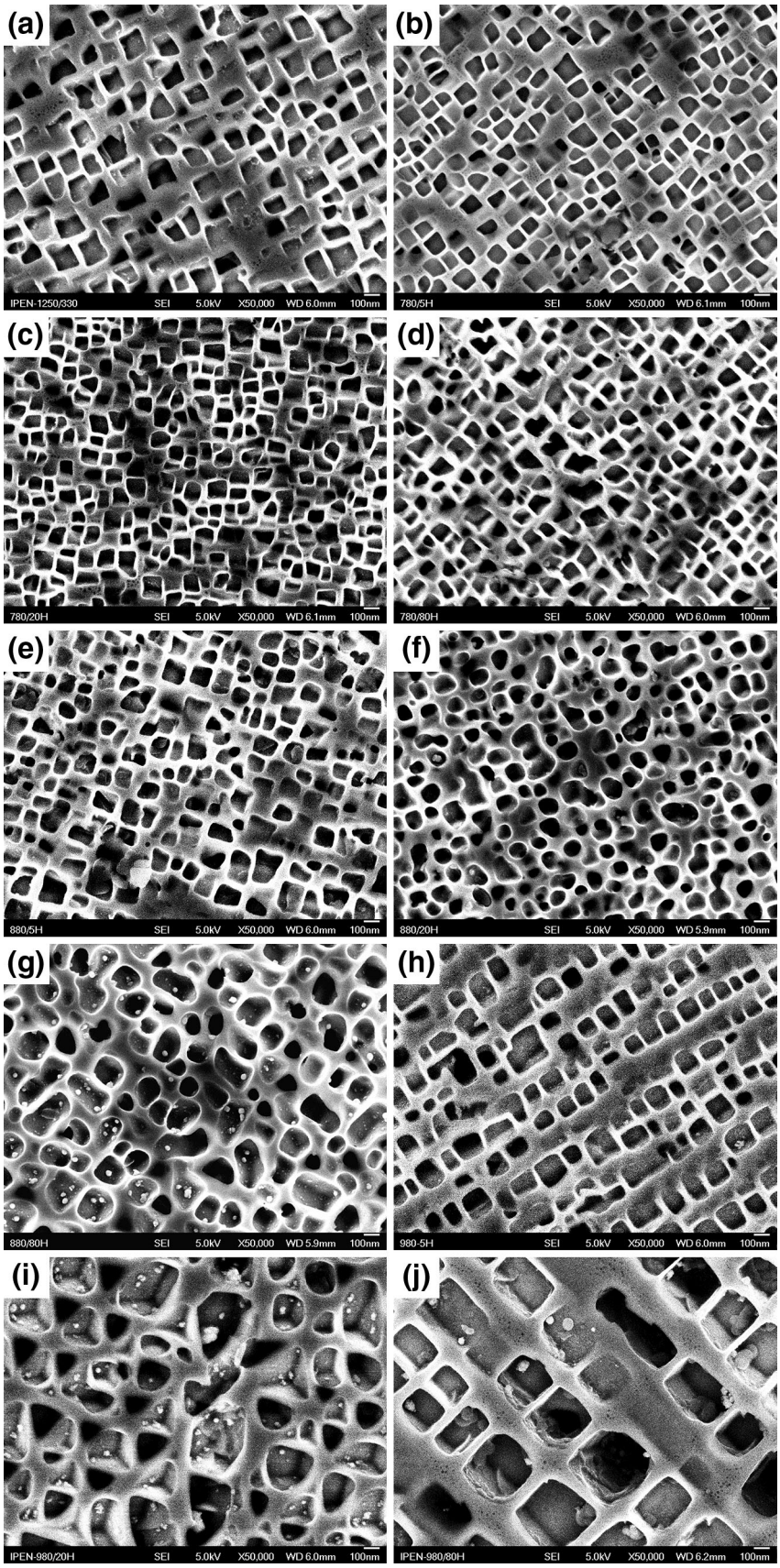

homogeneous material composed by γ (matrix), MC carbides and possibly borides (according to JMatPro simulations). The γ' precipitates observed in Fig. 6 were formed via solid-state reaction during air cooling of the samples. When the sample is air-cooled from the solutioning temperature, the solubility of aluminum and titanium in nickel decreases and causes precip-

◀**Fig. 7** (a) Micrograph of the MAR-M246 superalloy solutioned at 1250 °C for 330 min. (b) Micrograph of the MAR-M246 superalloy solutioned at 1250 °C for 330 min and aged at 780 °C for 5 h. (c) Micrograph of the MAR-M246 superalloy solutioned at 1250 °C for 330 min and aged at 780 °C for 20 h. (d) Micrograph of the MAR-M246 superalloy solutioned at 1250 °C for 330 min and aged at 780 °C for 80 h. (e) Micrograph of the MAR-M246 superalloy solutioned at 1250 °C for 330 min and aged at 880 °C for 5 h. (f) Micrograph of the MAR-M246 superalloy solutioned at 1250 °C for 330 min and aged at 880 °C for 20 h. (g) Micrograph of the MAR-M246 superalloy solutioned at 1250 °C for 330 min and aged at 880 °C for 80 h. (h) Micrograph of the MAR-M246 superalloy solutioned at 1250 °C for 330 min and aged at 980 °C for 5 h. (i) Micrograph of the MAR-M246 superalloy solutioned at 1250 °C for 330 min and aged at 980 °C for 20 h. (j) Micrograph of the MAR-M246 superalloy solutioned at 1250 °C for 330 min and aged at 980 °C for 80 h

Table 2 γ/γ′ mismatch for MAR-M246 superalloy at the aging temperatures

Aging temperature, °C	Lattice Mismatch, %
780	−0.145
880	−0.258
980	−0.278

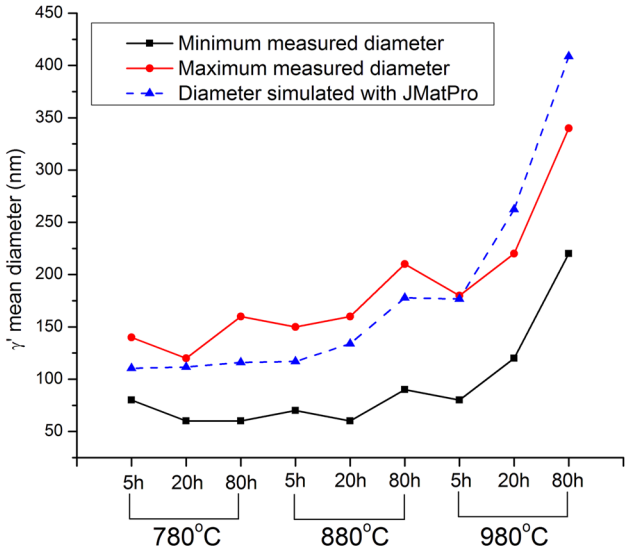

Fig. 8 Simulated (JMatPro software) and minimum/maximum measured values of the γ′ mean diameter as a function of aging conditions (time and temperature)

itation of fine γ′ particles. The sample solutioned at 1250 °C for 330 min presented cubic γ′ precipitates uniformly distributed with approximately 110 ± 20 nm in size.

3.4 Microstructural Characterization of Aged Samples

The equilibrium volume fraction of γ′ precipitated during aging is dictated by thermodynamics. Figure 7(a) shows higher magnification γ′ precipitates in the sample solutioned at 1250 °C for 330 min while Fig. 7 (b-j) shows micrographs

Table 3 Hardness of MAR-M246 superalloy after different aging heat-treatments

Temperature, °C	Time, h	Hardness, HV
780	5	465 ± 17
	20	488 ± 21
	80	481 ± 14
880	5	446 ± 18
	20	439 ± 10
	80	444 ± 14
980	5	431 ± 10
	20	400 ± 12
	80	399 ± 16

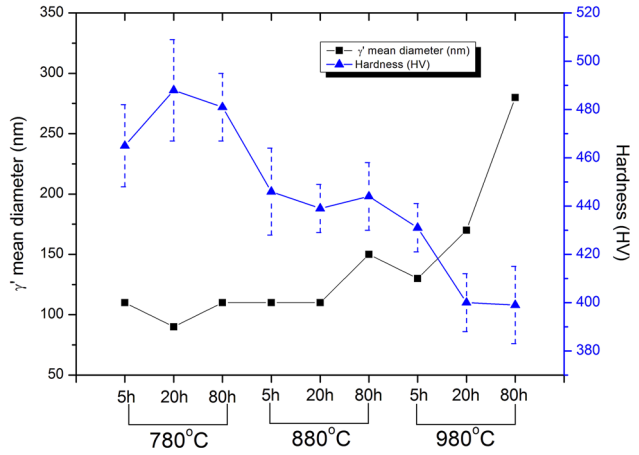

Fig. 9 Comparison between γ′ mean diameter and hardness values for the aged samples

from samples aged at different conditions after solution at 1250 °C for 330 min. The γ′ precipitates present in all aged samples are uniformly distributed in the γ matrix.

The morphology of the precipitates depends on the value of the γ/γ′ mismatch at the aging temperature. Table 2 shows the γ/γ′ mismatch calculated with JMatPro software for MAR-M246 superalloy at the aging temperatures. A near zero mismatch will induce a more round shape and a mismatch (negative or positive) different of zero will lead to a more cuboidal shape. Higher is the mismatch amplitude, more cuboidal is the precipitate shape.

It can be seen that the morphology and size of the precipitates from the aging at 780 °C are almost comparable with the as-solutioned sample, whatever the duration of the aging treatment. The aging treatments at 780 °C have no effect on the morphology and size of the precipitates as the temperature is too low to induce significant evolution of the microstructure. However, the aging treatments at 880 °C and 980 °C, in spite of higher lattice mismatch, clearly induce changes in size and/or morphology of the precipitates, as these temperatures are sufficiently high to activate significant coarsening (Ref 14).

Figure 8 shows both simulated (JMatPro software) and minimum/maximum measured values of γ′ mean diameter as a function of aging conditions (time and temperature). The initial γ′ particles mean diameter for simulations was 110 ± 20 nm,

which corresponds to the measured mean diameter in solutioned sample (Fig. 6b). For 780 and 880 °C, the simulated values are between the minimum and the maximum measured values. Additionally, samples heat-treated at 780 and 880 °C for 5, 20 and 80 h have not shown significant differences in the mean γ′ size when compared to the solutioned sample, in agreement with the low γ′ coarsening rates calculated with the aid of JMatPro software at these temperatures (14.2 nm/h$^{1/3}$ at 780 °C and 37.7 nm/h$^{1/3}$ at 880 °C). However, at 980 °C the simulated values were slightly higher than those measured for 20 and 80 h. A significant increase in the γ′ coarsening rate is observed at 980 °C, evidenced by the large mean size of these particles after 80 h of aging heat-treatment (Fig. 7j). The γ′ coarsening rate at 980 °C is 94.2 8 nm/h$^{1/3}$, 6.6 and 2.5 times higher than those at 780 and 880 °C, respectively.

3.5 Hardness Measurements

Table 3 shows the hardness values of MAR-M246 superalloy after different aging heat-treatments. The hardness of as-cast and solution heat-treated (1250 °C for 330 min) was 381 ± 12 and 415 ± 20 HV, respectively. It shows that the hardness did not vary significantly between the as-cast and heat-treated samples. Figure 9 shows the comparison between the γ′ mean diameter and the hardness values for the aged samples. It can be seen a tendency of lower hardness values for higher aging temperature, which should be mainly related to higher γ′ particle sizes at higher temperature.

4. Conclusions

The results of this investigation concerning the MAR-M246 nickel-based superalloy have led to the following data:

- the γ′ solvus, solidus and liquidus temperatures calculated with JMatPro software were 1181, 1317 and 1361 °C, respectively;
- the microstructure of the as-cast material presented a segregated dendritic microstructure and MC carbides with high aspect ratio and composed mainly by Ti, Cr, Mo, Ta, W;
- the microstructure of the alloy heat-treated at 1250 °C at 330 min showed a very homogeneous γ matrix with carbides and cubic γ′ precipitates uniformly distributed with approximately 110 ± 20 nm in size;
- the mean γ′ size of aged samples at 780 and 880 °C for 5, 20 and 80 h did not present significant differences when compared to the solutioned sample. However, a significant increasing in the γ′ particles was observed at 980 °C, evidenced by the large mean size of these particles after 80 h of aging heat-treatment.
- The hardness of as-cast and solution heat-treated (1250 °C for 330 min) was 381 ± 12 and 415 ± 20 HV, respectively. It can be seen a tendency of lower hardness values for higher aging temperature, which should be mainly related to higher γ′ particle sizes at higher temperature.

References

1. Allen F. Denzine, Thomas A. Kolakowski, and J.F. Wallace, Method of Improving Fatigue Life of Cast Nickel Based Superalloys and Composition. Patent US4078951-A. 1978
2. J.R. Davis, Ed., *ASM Specialty Handbook, Heat-Resistant Materials*, ASM International, Materials Park, 1997
3. M.H. Johnston, P.A. Curreri, R.A. Parr, and W.S. Alter, Superalloy Microstructural Variations Induced by Gravity Level During Directional Solidification, *Metall. Trans. A*, 1985, **16A**, p 1683–1687
4. R.C. Kramb, M.M. Antony, and S.L. Semiatin, Homogenization of a Nickel-Base Superalloy Ingot Material, *Scripta Mater.*, 2006, **54**, p 1645–1649
5. K.L. Zeisler-Mashl, and B.J. Pletka, Segregation During Solidification in the MAR-M247 System. *International Symposion on Superalloys, Pennslyvania*, *1992*, p. 175–184
6. S.R. Hegde, R.M. Kearsey, and J.C. Beddoes, Designing Homogenization-Solution Heat Treatments for Single Crystal Superalloys, *Mat Sci and Eng A*, 2010, **527**, p 5528–5538
7. I.M. Wolff, Precipitation Accompanying Overheating in Nickel-Base Superalloy, *Mater. Charact.*, 1992, **29**, p 55–61
8. A. Plati, Modelling of γ′ Precipitation in Superalloys. 2003. Dissertation (Master of Science). Department of Materials Science and Metallurgy, University of Cambridge, Cambridge, 2003
9. I.S. Kim, B.G. Choi, S.M. Seo, D.H. Kim, and C.Y. Jo, Influence of Heat Treatment on Microstructure and Tensile Properties of Conventionally Cast and Directionally Solidified Superalloy CM247LC, *Mater. Lett.*, 2008, **62**, p 1110–1113
10. S.A. Sajjadi, S.M. Zebarjad, R.I.L. Guthrie, and M. Isac, Microstructure Evolution of High-Performance Ni-base Superalloy GTD-111 with Heat Treatment Parameters, *J. Mater. Process. Technol.*, 2006, **175**, p 376–381
11. C.M. Kuo, Y.T. Yang, H.Y. Bor, C.N. Wei, and C.C. Tai, Aging Effects on the Microstructure and Creep Behavior of Inconel 718 Superalloy, *Mater. Sci. Eng. A*, 2009, **510**, p 289–294
12. W.F. Smith, *Structure and Properties of Engineering Alloys*, Mc-Graw Hill, New York, 1981
13. M. Bauccio, Ed., *ASM Metals Reference Book*, 3rd ed., ASM International, Materials Park, 1993
14. P. Caron and T. Khan, Improvement of Creep Strength in a Nickel-Base Single-Crystal Superalloy by Heat Treatment, *Mater. Sci. Eng.*, 1983, **61**, p 173–184